Mapping variation in radon potential both between and within geological units

J C H Miles* and J D Appleton**

* Health Protection Agency, Radiation Protection Division (HPA),
Chilton, Didcot, Oxon OX11 0RQ, UK
** British Geological Survey (BGS), Keyworth, Nottingham NG12 5GG, UK

Corresponding author: Jon Miles, jon.miles@hpa-rp.org.uk

Short title: Mapping radon variation between and within geological units

ABSTRACT

Previously, the potential for high radon levels in UK houses has been mapped either on the basis of grouping the results of radon measurements in houses by grid squares or by geological units. In both cases, lognormal modelling of the distribution of radon concentrations was applied to allow the estimated proportion of houses above the UK radon Action Level to be mapped. This paper describes a method of combining the grid square and geological mapping methods to give more accurate maps than either method can provide separately. The land area is first divided up using a combination of bedrock and superficial geological characteristics derived from digital geological map data. Each different combination of geological characteristics may appear at the land surface in many discontinuous locations across the country. HPA has a database of over 430,000 houses in which long-term measurements of radon concentration have been made, and whose locations are accurately known. Each of these measurements is allocated to the appropriate bedrock-superficial geological combination underlying it. Taking each geological combination in turn, the spatial variation of radon potential is mapped, treating the combination as if it was continuous over the land area. All of the maps of radon potential within different geological combinations are then combined to produce a map of variation in radon potential over the whole land surface.

1. Introduction

Exposure to radon indoors is the largest contributor to the radiation exposure of the population. It is also a highly variable contributor, the average indoor radon concentration varying by more than an order of magnitude between different areas. In order to prevent members of the public receiving high exposures to radon, it is necessary to identify those areas most at risk of high levels. This allows surveys of radon in existing houses to be directed to those areas where high radon levels are most likely to be found, and also allows building regulations in those areas to be altered to prevent new houses having high radon levels.

Maps of indoor radon levels are a convenient method of identifying the areas at risk. Such maps cannot be used to predict the radon level in an individual building, because radon levels can vary widely between apparently identical buildings located on the same geological unit. Maps can, however, give estimates of the mean radon levels in buildings by area. In addition, maps showing the geographical variation in the probability that new or existing buildings will exceed a radon reference level are particularly useful for directing action to prevent excessive exposures to radon. The more accurate the maps are, both in outlining the areas and in estimating the magnitudes, the better authorities and individuals can take appropriate decisions and target funding.

Indirect indicators of indoor radon are sometimes used to derive maps of radon prone areas (e.g. Kemski et al 2001; Mikšová and Barnet 2002; Appleton and Ball 2002). The indicators include parameters such as concentration of radium or radon in the ground, and permeability. But since the purpose of the maps is to estimate average radon levels in buildings (or the probability that the concentration will exceed a reference level), results of actual measurements of radon in buildings are the most directly relevant data. Soil gas radon, gamma spectrometry and soil permeability data have not been used to compile the radon potential maps described in this paper.

Various types of area boundary have been used in the analysis of house radon data and in presentation of maps, for example administrative boundaries, geological boundaries or arbitrary divisions such as grid squares. Use of administrative boundaries has the advantage of simplifying any subsequent administrative action, but radon potential may

vary widely within such boundaries, leading to misapplication of resources if radon maps are based on administrative boundaries. Geological boundaries delineate differences in radon potential much more closely than other types of boundary, though there is also variation in radon potential within geological units (Miles and Appleton, 2000). For instance, the Lower Lias in the county of Somerset, England comprises a complicated sequence of mudstones and thin limestones which are not differentiated on the 1:50,000 scale geological maps. Those parts of the Lower Lias with a greater proportion of limestone beds tend to have higher radon potential than those areas with few limestone beds (Figure 1; Appleton and Miles 2002).

Use of grid squares to group radon house data for mapping has the advantages that it allows an appropriate size of area to be chosen and it simplifies the analysis, but this method may also ignore important variations in radon potential within the squares. A grid square in Somerset, for example, contains Tournaisian Limestone (27-30%>AL), conglomeratic marginal facies of the Mercia Mudstone Group (3-4%>AL) and mudstones of the Mercia Mudstone Group (<0.1%>AL) (Figure 2).

In the UK, the National Radiological Protection Board (NRPB, now the Radiation Protection Division of the Health Protection Agency, HPA) has mapped the potential for high radon levels in houses by grid squares (Miles et al 1993, Miles 1988, Miles et al 1999, Green et al 2002), based on the results of radon measurements in houses. The British Geological Survey (BGS) has mapped radon potential using the same house radon data, but grouped according to the underlying geological units (Miles and Appleton 2000). Both of these mapping methods ignore some part of the geographical variation in radon potential: grid square mapping ignores variation between geological units within grid squares, and geological mapping ignores variation within geological units (or within areas sharing combinations of geological characteristics). The work reported in this paper describes an integrated radon mapping method that takes into account variations in radon potential both between and within geologically defined areas.

2. The principle of the integrated mapping method

In the integrated method, each geological combination is taken in turn, and the spatial variation of radon potential within the combination is mapped, treating it as if the combination was continuous over the land area. The following example is based on a hypothetical map of four geological units, shown in Figure 3. When the units were originally laid down, each was continuous, but parts of each unit have since been removed by erosion, and parts are now overlain by other units (see cross-section in Figure 4). The purpose of the exercise is to map the varying radon potential of each unit, starting, for example, with unit C.

The first step is to identify the locations of all measurement results, and separate out those located where the geological unit at the surface is C (shown as triangles in Figure 3). The measurements on unit C are distributed patchily across the area of the map, because in most places C is overlain by other units or has been removed by erosion. Nevertheless, the radon potential of C will be mapped as if C was continuous across the whole map area (which it was when it was laid down).

The grid square mapping procedure (described later) estimates the radon potential for each grid square, using only results from unit C. This produces Figure 5, where the different shadings represent different radon potentials.

However, unit C appears at the surface only in certain areas, so it is necessary to cut out the map in Figure 5 using the outline of unit C from Figure 3. This produces Figure 6. Unshaded areas of this map are areas where geological units other than C are at the surface.

The procedure is then repeated for the other geological units, filling in the blanks in Figure 6. The completed map shows variation both between and within geological units. Some of the borders between areas with different radon potential are defined by the boundaries of geological units, and some are defined by the edges of grid squares.

3. House radon data

The measurements of radon in houses used in this mapping exercise were carried out using small closed passive etched-track detectors, as described by Hardcastle et al (1996), or

very similar detectors. Surveys were carried out by post, with two detectors issued to each house. Householders were asked to place these in the main living area and an occupied bedroom. Measurements were carried out over 3 or 6 months. Questionnaires were provided to obtain details of detector placement, house type, and characteristics of houses, which could influence radon levels, such as double-glazing.

Since indoor radon levels are usually higher in cold weather, the results reported to householders are normalised for typical seasonal variations in radon levels to allow the estimated annual radon concentration to be reported (Wrixon et al 1988, Pinel et al 1995). It has been shown (Miles 1988) that the seasonal variations are correlated with average outdoor temperature variations. To allow for the fact that weather patterns vary from year to year, the annual average radon concentrations in houses used in this study were calculated using temperature corrections rather than seasonal corrections.

NRPB has carried out various surveys of radon in houses since the early 1980s, most of them funded by the Department of the Environment, Food and Rural Affairs. This has resulted in a database of radon levels in nearly half a million UK houses. The current mapping exercise is confined to England and Wales, for which over 430,000 house radon results were available. No other country has house radon data of this quantity and quality in a single repository.

Analysis of variance has demonstrated that geological unit, house type, double-glazing, floor level of bedroom and living area, and date of building year explain 29 % of the total variation (Hunter et al 2005). The analysis of the effects of geology (geological unit) and of house-specific factors showed that geological unit explained about 20% of the variation in logged radon levels in a data set for around 40,000 dwellings. Factors such as house type, double-glazing, date of construction, floor level of bedroom, and floor level of living room explained smaller percentages of the variation (3.8%, 2.3%, 1.1%, 1.1% and 1.0% respectively). The remaining three house specific factors (floor type, ownership, and draught proofing) only accounted for an extra 0.4% of the total variation. Indoor radon measurement data could be corrected to the equivalent concentration for a “standard” house. However, if this “standard” house data were to be used in mapping, then these house-specific factors would significantly affect the variability in maps. In the late 1990’s the UK government requested that actual house data rather than “standard” house data

should be used by NRPB and BGS for radon mapping. This is because government did not wish to have one radon map indicating the actual proportion of dwellings above the UK Action Level and another map indicating the radon potential of the ground.

4. Allocation of houses to geological combinations

In order to determine which geological unit a house lies on, it is necessary to know its location as accurately as possible. Ordnance Survey ADDRESS-POINT® locates houses on the national grid to an accuracy of 0.1 metres if the full address is known and it corresponds with an address in the ADDRESS-POINT® database. It was possible to obtain ADDRESS-POINT® coordinates for 81% of the houses in England and Wales with radon measurement results. For the other 19%, coordinates were obtained from Ordnance Survey Code-Point®, which allocates coordinates according to the postcode of a house. In the UK each postcode covers 15 homes on average, but in densely populated areas the number is higher and in sparsely populated areas it is lower. In most cases the grid reference allocated to a house using Code-Point® will be accurate to within a few hundred metres, but in sparsely populated areas the error may be greater. It would be preferable to exclude data for which the location is less accurately known, but this would lead to some geological combinations having too few results to allow the integrated mapping method to be applied.

Bedrock and superficial geological codes were attributed to each house location using the BGS 1:50,000 scale DiGMapGB digital data. Geological mapping of the UK has been carried out over many years during which time there have been changes in the nomenclature of mapped rock units. Consequently, the names of geological units sometimes change at map sheet boundaries. In order to facilitate the seamless 1 km interpolation of radon potential within major geological units, simplified bedrock and superficial geology classification systems were developed which ensures continuity across map sheet boundaries and also groups some geological units with similar characteristics. Grouping similar geological units ensured that there were a sufficient number of indoor radon measurements for intra-geological unit grid square mapping to be carried out over a greater proportion of the UK. There are nearly 4500 named bedrock geological units in England and Wales and these were grouped using a simplified bedrock classification comprising only 406 units (Appleton 2005). For example, 333 individually named Visean limestones were all grouped as VIS-LMST for intra-geological unit radon potential

mapping. The 888 individually named 1:50,000 scale superficial geology units were grouped according to a simplified system based on permeability and genetic type (Table 1).

5. Mapping variations in radon potential within geological combinations

Within each geological combination with more than 100 radon measurements, the variation of radon potential was mapped using 1 km squares of the national grid. A radon potential was allocated to each 1 km grid square on the basis of the nearest 30 house radon measurement results to that square, or all of the results in the square if that was 30 or more. This number of measurements was chosen on the basis of trials with a model data set, described in Miles (2002). The method can be summarised as follows:

Taking each grid square in turn as a target square,

1. If there are 30 results or more within the target square, use all of these results and no others.
2. Otherwise, gradually expand a circle out from the centre of the square until it encompasses 30 results.
3. Calculate the geometric mean (GM) and geometric standard deviation (GSD) of the results.

Use the GM and GSD in a lognormal model to estimate the proportion of the distribution above the Action Level. Allocate that proportion to the target square.

There were some differences between the method as described in Miles (2002) and the application of the method in this work. These are described in the following subsections.

5.1 Maximum distance from target square for data collection

Miles (2002) set a maximum distance of 5 km from the centre of the target square for collection of house radon data. This restriction was applied because the mapping method was originally intended for mapping radon potential irrespective of geological boundaries. The restriction was intended to reduce the number of radon results collected from different geological units from the target square, which could have very different radon potential. When mapping a single geological combination, which should have less lateral variation in radon potential than when no distinction is made between geological units, this restriction was considered unnecessary, and was removed. Thus data at any distance from the target square can contribute to the target square estimate.

5.2 Use of unsmoothed geometric means

Miles (2002) used smoothed geometric means when calculating the proportion of homes above the UK Action Level to avoid the appearance of artefacts where random variations in radon levels would mislead those using the map into thinking there were real variations in radon potential. The unsmoothed estimates are more accurate, but smoothing was used as a compromise between the desire to show all possible genuine variation in radon potential and the need to avoid showing false variations. This precaution is unnecessary in the combined mapping described here, because changes in radon potential at the boundaries between geological combinations make such artefacts much less noticeable.

5.3 Bayesian estimation of GSD

It has been shown (Miles 1998) that when UK house radon results are grouped by 1 km grid square, the mean GSD is 2.5, with no significant variation of GSD with GM. For the 1 km grid square mapping method used here, 30 results are available for most squares for the estimation of GM and GSD. Thirty results are not sufficient to allow the accurate estimation of GSD, but where the numbers of results are limited, and the expected distribution of GSDs is known, Bayesian statistics can improve estimates of GSDs for individual areas (see Appendix).

Whereas the uncertainty of a radon potential estimate is higher when based on smaller number of measurements (Miles and Appleton 2000), the use of Bayesian estimates of GSD gives less uncertain estimates and does not bias the estimates in any way. The reduction of the uncertainty by the use of Bayesian statistics was significant but not very large (Figure 7). This is because the geometric mean radon value has a much greater influence on radon potential estimates than the GSD.

5.4 Correction of GSD for year-to-year variability in radon levels

It has been shown (Darby, 2003) that the measured GSD for any group of house radon measurement results, each made over a few months, is higher than the GSD that would have been observed if the measurements had been made over several years in each house. The difference is caused by uncertainties in estimates of long-term average radon concentrations, both from extrapolating from 3 or 6 months to a year, and from year-to-

year variations in radon levels. It is possible to correct measured GSDs for this effect, using data from studies of the year-to-year variation in 3 or 6 month house radon measurement results. Such corrections always reduce GSDs, and therefore always reduce percentages above a threshold, if the GM of the area is below the threshold. Earlier mapping exercises, in the UK and elsewhere, did not take account of this factor.

5.5 Mapping radon potential for combinations with few measurements

About 20% of homes in the UK are located on geological combinations for which the indoor radon data are too sparse to allow the integrated mapping method to be applied. In cases where there are too few house radon results attributed to a geological combination to allow the spatial variation to be mapped using the method described above, the average radon potential for all the houses on the combination is estimated and applied to the whole combination in each 100 km grid square of the British National Grid. Some combinations have too few results to allow radon potential to be calculated directly, and in these cases the data for similar combinations are grouped together, or radon potential is assigned by analogy with similar combinations.

6. Results of the mapping

All of the radon potential data for different geological combinations were combined to produce a map of variation in radon potential over the whole land surface (see extract in Figure 8).

The results of the integrated mapping method allowed significant variations in radon potential within bedrock geological units to be identified, such as in the radon prone Jurassic Northampton Sand Formation (NSF). Moderate radon potential (<4%>AL) occurs within and to the northwest of the urban centre of Northampton with much higher potential (>12%>AL) to the north (Figure 9) and also in the nearby urban centres of Wellingborough and Kettering (Appleton et al 2000; Miles and Appleton 2000). These variations are significant because they are based on a large number of radon measurements (Figure 10). The NSF comprises a lower ironstone, often with a uraniferous and phosphatic nodular horizon at the base (Sutherland 1991), overlain by a massive yellow or brown

calcareous sandstone (locally called the “Variable Beds”, Hains and Horton 1969). Variable Beds sandstones at Harlestone Quarry (HQ, Figure 9) contain on average 11% Fe_2O_3T, 0.37% P_2O_5 and 1.1 mg kg^{-1} uranium (Hodgkinson et al 2005) in an area with a radon potential of about 3%>AL whereas at Pitsford Quarry (PQ, Figure 9), the ironstones contain 29% Fe_2O_3T, 1.0% P_2O_5 and 2.4 mg kg^{-1} uranium in an area with radon potentials in the range 8 – 21%>AL. The Variable Beds are found only in the immediate vicinity of Northampton and are largely missing from the Kettering and Wellingborough areas, which may explain why the radon potential for the NSF is higher in these areas compared with the Northampton urban area. Radon in soil gas correlates positively (r = 0.88, p 0.0005) with the radon potential of the NSF (Figure 11), and there is also a close correlation (r=0.86, p 0.0005) between radon emanation and uranium in rock samples (Figure 12). Track etch alpha autoradiography studies indicate that uranium is associated predominantly with the goethite-rich clay matrix of the ironstones, and is also concentrated in occasional phosphatic nodules (Hodgkinson et al 2005).

Geological radon potential mapping based on the average radon potential for a geological unit within a 1:50,000 scale map sheet failed to identify that a sector of the Carboniferous Limestone to the NE, E and SE of Buxton in Derbyshire has a radon potential that appears to be significantly lower than the very high potential (>30% >AL) that characterises much of the Derbyshire Dome (Figure 13). The moderate radon potential associated with the sector to the east of Buxton is broadly compatible with an area of lower estimated uranium (eU, Figure 14) determined from the airborne gamma spectrometric ^{214}Bi photopeak intensity (Jones et al 2005). The reason for this variation is not entirely clear but may be related to the distribution of residual soil enriched in radium. However, detailed correlation between spatial patterns on airborne eU images and radon potential maps is difficult to establish because (1) the differences in the interpolation methods used for the airborne gamma spectrometric and indoor radon data and (2) the generally uneven distribution of indoor radon measurements away from the main urbanised areas (Figure 15). Airborne eU data reflects the ^{214}Bi concentration (and hence ^{222}Rn concentration) only in the upper 0.3 m of the soil profile, although much of that radon will have originated at greater depths, and is likely to affect radon levels in houses.

Grouping radon measurements data by geology and 1 km grid square has also led to the identification of new radon affected areas that it was not possible to identify using only grid square mapping, especially in those areas where there were few radon measurements, such as the Gower Peninsula in south Wales (Appleton and Miles 2005).

7. Difficulties encountered in mapping

In areas of low measurement density, clusters of high results can influence the map over a relatively wide area. It is difficult to avoid this, since the designations of radon potential are based on the best available evidence: the nearest radon results on the same geological combination.

A cluster of high radon measurement results in an area with both generally low results and a low measurement density will affect the estimated proportion above the Action Level over a wide area. This problem is illustrated in the Lutterworth area where there are 380 measurement results on glacial till overlying Jurassic Lower Lias bedrock units, with 261 of the measurements being in the town of Lutterworth (Figure 16a; note that each dot signifies a post code location and multiple measurements may be available for a postcode). Measurements located on the southeast side of the town are much higher than the results elsewhere, with 19 results over 100 Bq m^{-3} within 500 metres of each other, and other moderately high results nearby. The position of the high results produces a large area of high (>8%) radon potential for this geological combination spreading out southeast from Lutterworth (Figure 16b). The extent of the high radon potential area to the SE of Lutterworth is reinforced by occasional high radon results further southeast of Lutterworth. These include some above 100 Bq m^{-3} about 2 and 7 km to the SE of the town centre. This area of high radon potential is difficult to explain geologically. Glacial till overlying Lower Lias mudstone with subsidiary limestone bedrock normally has a relatively low radon potential (<2%>AL). 1:10,000 geological and historical (1896 and 1904) Ordnance Survey map data do not provide an obvious explanation for the high radon values to the SE of Lutterworth or in the southern half of Lutterworth town, although it is possible that some significant geological feature may have been missed in areas where the land is covered by private houses and gardens and when there is no borehole or site investigation information available. Additional measurements are required to resolve whether this area of high radon potential is ‘real’ or is partly an artefact of the mapping method. Restricting

the distance over which measurements are permitted to contribute to a radon potential estimate for a geological combination within a 1 km grid square would restrict the extent of high radon areas caused by a restricted cluster of high indoor radon measurements. However, this would leave many grid squares with no estimates and these would have to be infilled using the average radon potential for each geological combination.

8. Averaging over grid squares

The mapping method discussed here produces highly detailed maps, in which one street may include houses in several different radon potential categories. This causes difficulties in presentation, in particular because printing maps covering England and Wales, showing all of the detail mapped, would require hundreds of map sheets to be produced. One possible solution to this problem is to avoid producing paper maps at all, and offer the results of the mapping solely as a database to be queried for individual addresses or grid references. However, this has the serious disadvantage that it is not easy to gain an impression of the extent and nature of the radon problem for any area.

An alternative solution would be to average the radon potentials over standard areas, such as 1 km grid squares. This would allow the production of an atlas covering England and Wales, similar to the atlas produced previously by NRPB (Green et al 2002). This possibility was examined for a trial area, to discover whether averaging radon potentials over 1 km grid squares would cause a significant loss of information (Hunter 2005). The conclusion was that there would be a considerable loss of information, so this possibility was abandoned.

A third possibility for presenting the information is to produce a summary 1 km grid square map in which each square is allocated the highest radon potential category of any geological combination inside it. This could be produced as a convenient atlas covering England and Wales. The atlas would be backed up by a database as described earlier, which would allow the radon category of any individual house or development site to be determined. The advantage of this method of presentation is that for many grid squares no database enquiry would be necessary, as the atlas would show that the proportion of houses above the radon Action Level throughout the square was very low. The summary map

would also give a clear picture of where the areas of concern for indoor radon were located.

9. Uncertainties in maps of radon potential

There can be many sources of uncertainty and bias in the data underlying radon potential maps and in the processing methods used (NRPB-BGS 2004). For instance, the selection of houses for measurement may be biased, as volunteers and willing participants may have higher radon levels than reluctant participants (Miles 2001). The radon levels found in houses depend, among other factors, on building characteristics, which vary from area to area. There can also be significant uncertainties in the estimates of annual average radon concentrations in houses, particularly at lower radon levels. There are spatial uncertainties in the location of both houses and geological boundaries. Spatial uncertainties and uncertainties in the magnitudes of derived parameters, such as the proportion of houses above a threshold, are not independent: if a house is allocated to the wrong geological unit, its radon result distorts the estimated proportion above the threshold for that unit.

These factors make it very difficult to assign spatial and magnitude uncertainties to radon maps. For this reason, maps of radon potential do not normally carry information about uncertainties. Some informal testing of early UK maps of radon potential has been carried out, comparing the predicted percentage above the UK Action Level with the proportion found on later testing in the same area. These tests indicated that the predictions were consistent with the later measurement results over 5 km grid squares. However, such tests are far from definitive: both initial and later measurements could be subject to the same biases, and in any case the mapping methods have developed since the initial maps were made. Displaying spatial and magnitude uncertainties on maps in a manner which is meaningful to the users of the maps is also a difficult problem. A map showing the distribution of indoor radon measurements would provide some indication of uncertainty, but would be difficult to interpret because it could not show how the results were grouped for processing. There remains much to be done in this area.

10. Conclusions

A method has been developed that allows spatial variation in radon potential to be mapped, taking into account variations both between and within geological groupings. The

integrated mapping method imposes fewer, and more plausible, assumptions about the nature of the spatial variation in radon potential than earlier mapping methods. Nevertheless, it should be borne in mind that no map can fully reflect the detailed reality of variation in radon potential. The integrated mapping method has been applied to mapping radon potential in England and Wales (Miles et al 2005; Appleton and Miles 2005).

Acknowledgments

The authors thank I. Barnet (Czech Geological Survey), D.G. Jones (BGS), R.G.E. Haylock N. Hunter, G.M. Kendall, C.R. Muirhead and W. Zhang (HPA), R. Klingel (Kemski & Partner, Bonn, Germany) and R. Lehmann (Federal Office for Radiation Protection, Germany) for assistance and for suggesting improvements to the paper. JDA acknowledges permission to publish by the Executive Director, British Geological Survey (NERC).

References

Appleton JD 2005. Simplified geological classification for radon potential mapping in England, Wales and Scotland. British Geological Survey Internal Report, IR/05/086.

Appleton JD and Ball, TK 2002. Geological radon potential mapping. pp 577-613 in: Bobrowsky, P.T. (Editor) Geoenvironmental mapping: methods, theory and practice. Rotterdam: Balkema

Appleton JD Miles JCH and Talbot DK 2000. Dealing with radon emissions in respect of new development: Evaluation of mapping and site investigation methods for targeting areas where new development may require radon protective measures. British Geological Research Report RR/00/12.

Appleton JD and Miles JCH 2002. Mapping radon-prone areas using integrated geological and grid square approaches. 34-43 in Barnet I, Neznal M and Miksova J, Radon investigations in the Czech Republic IX & the Sixth International Workshop on the Geological aspects of Radon Risk Mapping, Prague: Czech Geological Survey.

Appleton JD and Miles JCH 2005. Radon in Wales. In: Nicol D and Bassett MG (Editors), Urban Geology of Wales, Volume 2. National Museum of Wales Geological Series. Cardiff.

Green BMR, Miles JCH, Bradley EJ and Rees DM 2002. Radon Atlas of England and Wales. UK: National Radiological Protection Board. NRPB-W26.

Darby SC 2003. Private communication. University of Oxford Clinical Trial Service Unit and Epidemiological Studies Unit.

Hains BA and Horton A 1969. British Regional Geology: Central England (Third edition). BRG10. British Geological Survey.

Hardcastle GD, Howarth CB, Naismith SP, Algar RA and Miles JCH 1996. NRPB etched-track detectors for area monitoring of radon. NRPB-R283.

Hodgkinson ES Jones DG, Emery C, and Davis JR 2005. Petrography and geochemistry of two East Midlands Jurassic Ironstones and their relationship to radon potential. British Geological Survey Research Report RR/05/041.

Hunter N, Howarth CB, Miles JCH and Muirhead CR. 2005. Year-to-year variations in radon levels in a sample of UK houses with the same occupants. 438-447 in: McLaughlin, JP, Simopoulos, ES, and Steinhäusler, F. (Editors), Seventh International Symposium on the Natural Radiation Environment (NRE-VII) Rhodes, Greece, 20-24 May 2002. Elsevier, 1575 pp.

Hunter N 2005. A Two-Error Component Model for Measurement Error: Application to Radon Concentrations. (in preparation)

Jones DG, Appleton JD, Davis JR, Emery C, Hodgkinson E, Rainey PP and Strutt MH 2005. The High Resolution Airborne Resource and Environmental Survey Phase 1 (Hi-RES-1): Evaluation and ground follow-up of radiometric data. British Geological Survey Internal Report, IR/05/060.

Kemski J, Siehl A, Stegemann R and Valdivia-Manchego M 2001. Mapping the geogenic radon potential in Germany. Science of the Total Environment, 272(1-3), 217-230.

Mikšová J and Barnet I 2002. Geological support to the National Radon Programme (Czech Republic). Bulletin of the Czech Geological Survey, 77(1), 13-22.

Miles JCH, Green BMR and Lomas PR 1993. Radon affected areas: Scotland. Documents of the NRPB, 4,6 1-8.Miles, JCH, 1998, Mapping radon-prone areas by lognormal modelling of house radon data. Health Physics 74, 370-378.

Miles JCH 1998. Development of maps of radon-prone areas using radon measurements in houses. Journal of Hazardous Materials, 61, 53-58.

Miles JCH, Green BMR and Lomas PR 1999. Radon affected areas: Northern Ireland - 1999 review. Documents of the NRPB, 10,4 1-8.

Miles JCH 2001. Sources of bias in data for radon potential mapping. In Proceedings of the Third Eurosymposium on Protection Against Radon, Liege 2001.

Miles JCH 2002. Use of a Model Data Set to Test Methods for Mapping Radon Potential. Radiation Protection Dosimetry 98, 211-218.

Miles JCH and Appleton JD. 2000. Identification of localised areas of England where radon concentrations are most likely to have >5% probability of being above the Action Level. DETR Report No: DETR/RAS/00. 001

Miles JCH, Appleton JD, Green BMR, Bradley EJ and Rees DM 2005. Atlas of radon potential in England and Wales. In preparation.

NRPB-BGS 2004. Uncertainties in integrated geological/grid square radon mapping. British Geological Survey Internal Report, IR/04/047. 65 pp.

Pinel J, Fearn T, Darby SC and Miles JCH 1995. Seasonal correction factors for indoor radon measurements in the United Kingdom. Radiation Protection Dosimetry 58, 127-132.

Sutherland DS 1991. Radon in Northamptonshire, England: geochemical investigation of some Jurassic sedimentary rocks. Environmental Geochemistry and Health, Vol. 13, No. 3, 143-145.

Wrixon AD, Green BMR, Lomas PR, Miles JCH, Cliff KD, Francis EA, Driscoll CMH, James AC and O'Riordan MC 1988. Natural radiation exposure in UK dwellings. NRPB R-190.

Appendix

Estimation of standard deviations of radon measurements for mapping (R Haylock, HPA, May 2002)

The problem of estimating the standard deviations of radon measurements for radon mapping is ideally suited to applying Bayesian statistical theory (Lee, 1989). Using this theory prior information about the variance in a grid square, based on the data from other similar grid squares, can be mathematically combined with the information provided by a sample of data from the square of interest to obtain an improved estimate. For ease of computation, this note considers the problem of estimating the variance of the logged radon concentrations in a grid square rather than the standard deviation. The variance is the square of the standard deviation

Method:

Note: all variances and standard deviations here are sample (not population) variances and standard deviations.

Let φ represent the unknown variance in the square of interest.

Let the prior information about the variance, φ, be expressed by an inverse chi squared distribution with mean *E* and variance *V*:

$$\varphi \sim S_0 \chi^{-2}_{\upsilon_0}$$

where

$$S_0 = 2E\left(1 + E^2/V\right) \qquad and \qquad \upsilon_0 = 4 + \frac{2E^2}{V}.$$

Let the logged radon measurements for the square of interest be defined as $\underline{x} = (x_1, \ldots, x_n)$.

Assume that these measurements are normally distributed, $N(\mu, \varphi)$, where μ, the mean of the distribution, is known. In reality the mean μ is unknown but can be sufficiently well approximated by the sample mean, $\overline{x}$, where

$$\overline{x} = \sum_{i=1}^{n} x_i / n.$$

Next, using $\overline{x}$, calculate the variable S as

$$S = \sum_{i=1}^{n} (x_i - \overline{x})^2$$

Using the values defined above an estimate for φ can be obtained by combining the prior information with the sample data, using Bayes theorem[1], to form a posterior distribution. The mean of the posterior distribution can be used as an estimate for φ.
The posterior distribution for φ is also an inverse chi squared:

$$\varphi \sim S_1 \chi^{-2}_{\upsilon_1}$$

where $S_1 = S_0 + S$ and $\nu_1 = \nu_0 + n$

The mean of this posterior distribution, $\hat{\varphi}$ is

$$\hat{\varphi} = \frac{S_0 + S}{\upsilon_0 + n - 2}$$

Example:

Sample: (logged values)

3.96, 2.41, 4.11, 4.61, 4.47, 3.39, 4.06, 4.22, 3.59, 3.82, 3.5 2.75, 3.32, 3.43, 3.93, 4.46, 5.64, 4.25

From the sample the following quantities are calculated:

$\overline{x}$ = 3.8844, n = 18, S = 9.08744

Prior information for the calculation was obtained from data on 908 1km grid squares. The GSD measurements from each square were squared to obtain the variance for each square. The mean and variance of the 908 variance measurements were then derived as

E = 0.85046615 and V = 0.07434262.

From E and V the quantities S0 and n0 were derived as: S0 = 18.249608; n0 = 23.458359.

The posterior estimate of the variance for the square was then calculated as $\hat{\varphi}$ = 0.6928076.

Expressing the GSDs in the original scale (Exp (GSD)) gives:

From the prior distribution: 2.51

From the sample data: 2.08

From the posterior distribution: 2.30.

Reference: Lee, PM. 1989. Bayesian Statistics: an introduction. Oxford University Press,

Table 1: Simplified superficial geology classification

Simplified superficial geology code	Explanation and dominant lithology	Number of named 1:50,000 scale units	Permeability
CALC	calcrete	12	impermeable
C-DMTN	clay with flints	4	impermeable
CLSI	clay-silt	234	impermeable
DMTN	diamicton (mainly glacial till)	77	impermeable
FRAG	rock fragments	4	permeable
H-CLSI	head (congeliturbate) deposits (clay-silt)	17	impermeable
H-DMTN	head (congeliturbate) deposits (diamicton)	10	impermeable
H-SAGR	head (congeliturbate) deposits (sand and gravel)	8	permeable
PEAT	peat	11	waterlogged in winter
SAGR	sand and gravel	511	permeable

FIGURE CAPTIONS

Figure 1: Variation of radon potential within the Lower Lias (limestone-mudstone) sequence in Somerset, England. (1 km grid mapping based on unweighted geometric mean (GM), geometric standard deviation (GSD) 2.26, smoothing ratio = 2; see Miles 2002 for explanation) Shading: white <1%; pale grey 1-3%; medium grey 3-10%, black >10% dwellings exceed the radon Action Level) (Copy of Figure 4, Appleton and Miles 2002).

Figure 2: Lateral variation in radon potential within a grid square in Somerset, England (see text for explanation; black grid = 1 km; Topography © Crown copyright. All rights reserved).

Figure 3. Map showing four geological units, with locations of radon measurements marked with different symbols for different geological units.

Figure 4. Cross-section of map in Figure 3.

Figure 5. The results of mapping the whole area using only the measurement results in unit C, marked with triangles.

Figure 6. The grid square shading in Figure 3 is cut out using the outline of geological unit C, to show the variation of radon potential within unit C.

Figure 7. Box and whisker plot showing the range of radon potential estimates for 300 random sub-samples of 10, 30 and 100 measurements from a population of 2007 radon measurements on the Northampton Sand Formation in a 5-km grid square (average radon potential = 11.8%). Bottom line of box = Lower quartile; Top line of box = Upper quartile; Middle line of box = Median; Lower (upper) whisker = maximum of (i) lower (upper) quartile plus 1.5 times the inter-quartile range and (ii) the minimum (maximum) observation; any values above upper whisker or below lower whisker are outliers and plotted individually. 1 = Subset size 10, Subset GSD used to estimate %>AL of subsets; 2

= Subset size 10, Bayesian GSD; 3 = Subset size 30, Subset GSD; 4 = Subset size 30, Bayesian GSD; 5 = Subset size 100, Subset GSD; 6 = Subset size 100, Bayesian GSD.

Figure 8. Provisional radon potential map of southwest England based on geology and indoor radon measurements.

Figure 9. Radon potential of ground underlain by the Northampton Sand Formation (but not covered by superficial deposits) in the Northampton area (HQ = Harlestone Quarry; PQ = Pitsford Quarry). Map based on geology and indoor radon measurements.

Figure 10. Number of indoor radon measurements used to estimate radon potential in each 1 km grid square underlain by the Northampton Sand Formation (but not covered by superficial deposits) in the Northampton area. Map based on geology and indoor radon measurements.

Figure 11. Relationship between average soil gas radon concentration (Bq L^{-1}) and the geological radon potential (Estimated proportion of dwellings exceeding the UK radon Action Level (200 Bq m^{-3})) for the Northampton Sand Formation. Data grouped by 5 km grid square (redrawn after Figure 3-28 in Appleton et al, 2000).

Figure 12. Relationship between radon emanation and uranium concentration of rock samples from the Northampton Sand Formation (Hodgkinson et al 2005)

Figure 13. Radon potential map of the northern part of the Derbyshire Dome underlain by Carboniferous limestone, not covered with superficial deposits. Map based on geology and indoor radon measurements.

Figure 14. eU (ppm) map of the northern part of the Derbyshire Dome underlain by Carboniferous limestone, not covered with superficial deposits. Data from Hi-RES-1 airborne gamma spectrometry survey (Jones et al 2005)

Figure 15. Maximum distance to furthest of 30 measurements used to estimate the radon potential for Carboniferous limestone with no superficial cover, northern sector of the Derbyshire Dome (max. distance <0.56 km indicates that 30 or more measurements occur within the 1 km grid square).

Figure 16. (a) Indoor radon measurement locations and maximum distance to furthest of 30 measurements used to estimate the radon potential for glacial till overlying Lower Lias bedrock (max. distance <0.56 km indicates that 30 or more measurements occur within the 1 km grid square); (b) radon potential map for glacial till overlying Lower Lias bedrock in the Lutterworth area (map based on geology and indoor radon measurements).

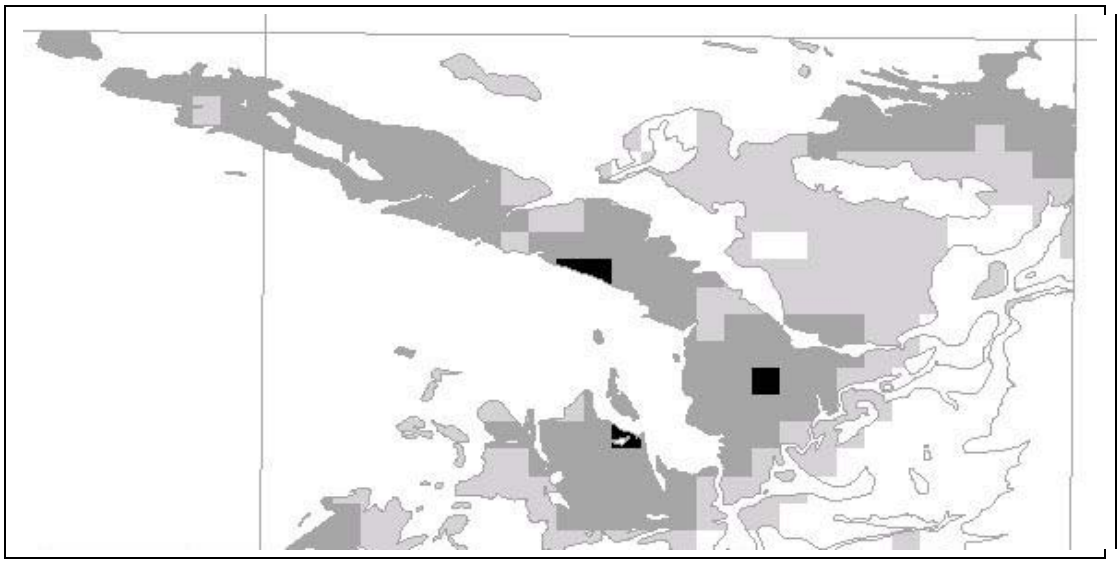

Figure 1: Variation of radon potential within the Lower Lias (limestone-mudstone) sequence in Somerset, England. (1 km grid mapping based on unweighted geometric mean (GM), geometric standard deviation (GSD) 2.26, smoothing ratio = 2; see Miles 2002 for explanation) Shading: white <1%; pale grey 1-3%; medium grey 3-10%, black >10% dwellings exceed the radon Action Level) (Copy of Figure 4, Appleton and Miles 2002).

Figure 2: Lateral variation in radon potential within a grid square in Somerset, England (see text for explanation; black grid = 1 km; Topography © Crown copyright. All rights reserved).

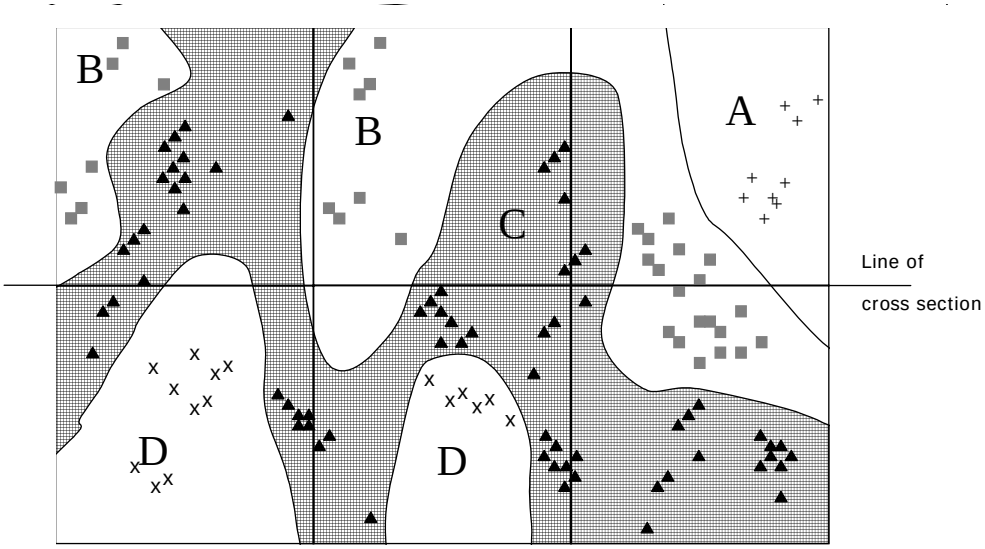

Figure 3. Map showing four geological units, with locations of radon measurements marked with different symbols for different geological units.

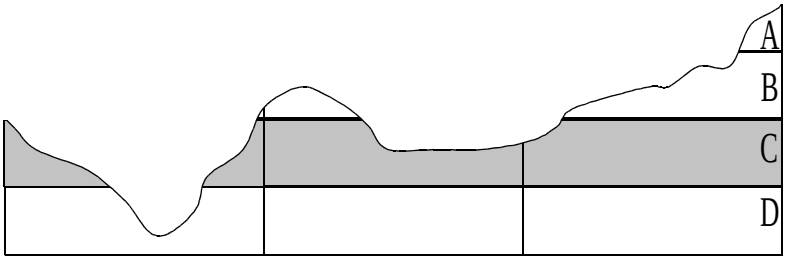

Figure 4. Cross-section of map in Figure 3

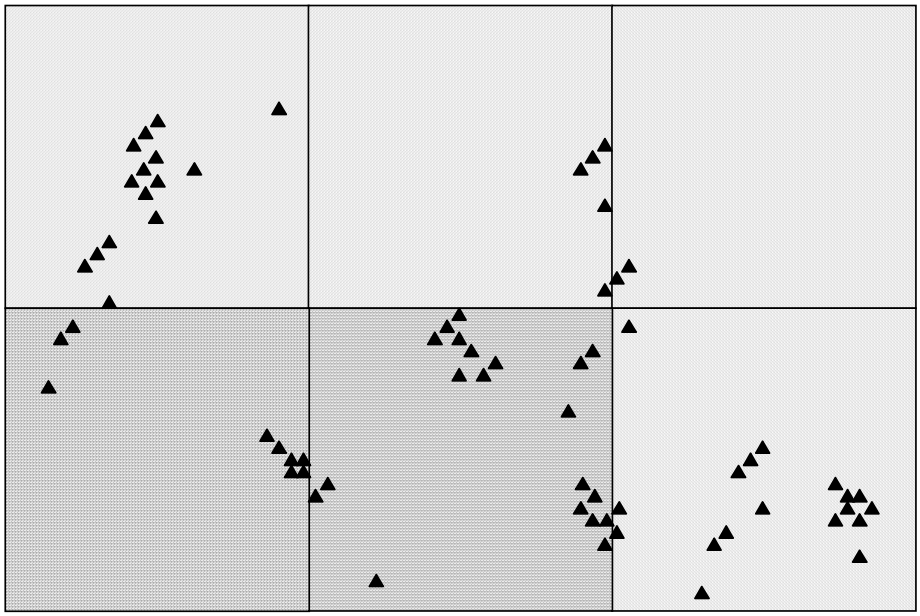

Figure 5. The results of mapping the whole area using only the measurement results in unit C, marked with triangles.

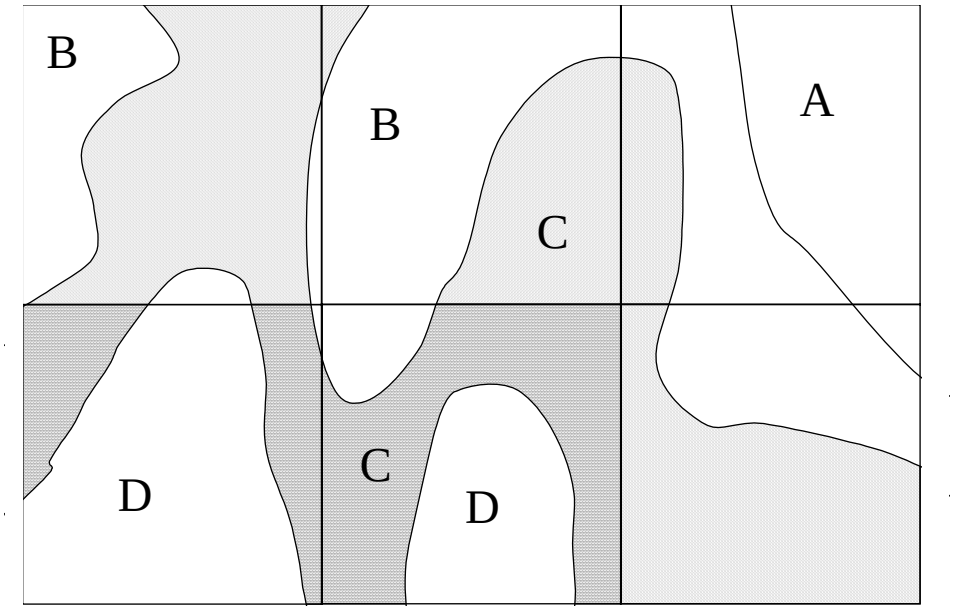

Figure 6. The grid square shading in Figure 3 is cut out using the outline of geological unit C, to show the variation of radon potential within unit C.

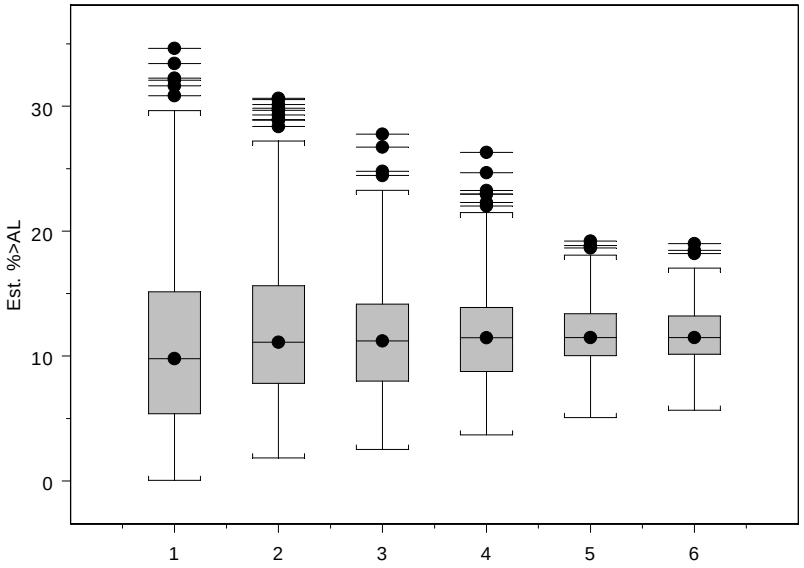

Figure 7. Box and whisker plot showing the range of radon potential estimates for 300 random sub-samples of 10, 30 and 100 measurements from a population of 2007 radon measurements on the Northampton Sand Formation in a 5-km grid square (average radon potential = 11.8%). Bottom line of box = Lower quartile; Top line of box = Upper quartile; Middle line of box = Median; Lower (upper) whisker = maximum of (i) lower (upper) quartile plus 1.5 times the inter-quartile range and (ii) the minimum (maximum) observation; any values above upper whisker or below lower whisker are outliers and plotted individually. 1 = Subset size 10, Subset GSD used to estimate %>AL of subsets; 2 = Subset size 10, Bayesian GSD; 3 = Subset size 30, Subset GSD; 4 = Subset size 30, Bayesian GSD; 5 = Subset size 100, Subset GSD; 6 = Subset size 100, Bayesian GSD.

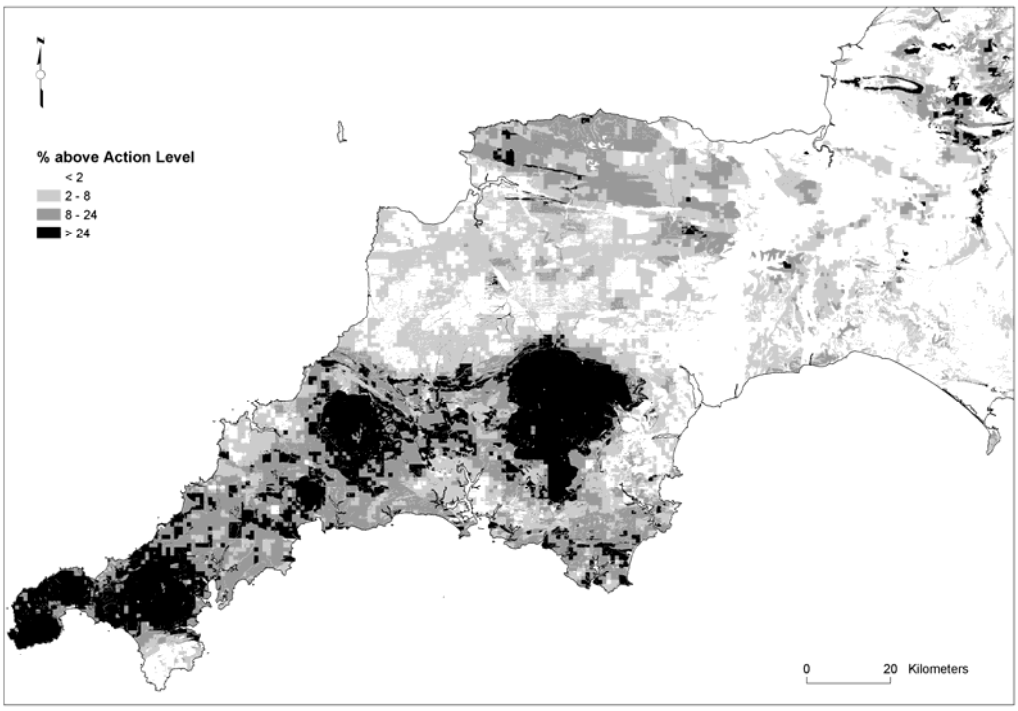

Figure 8. Provisional radon potential map of southwest England based on geology and indoor radon measurements.

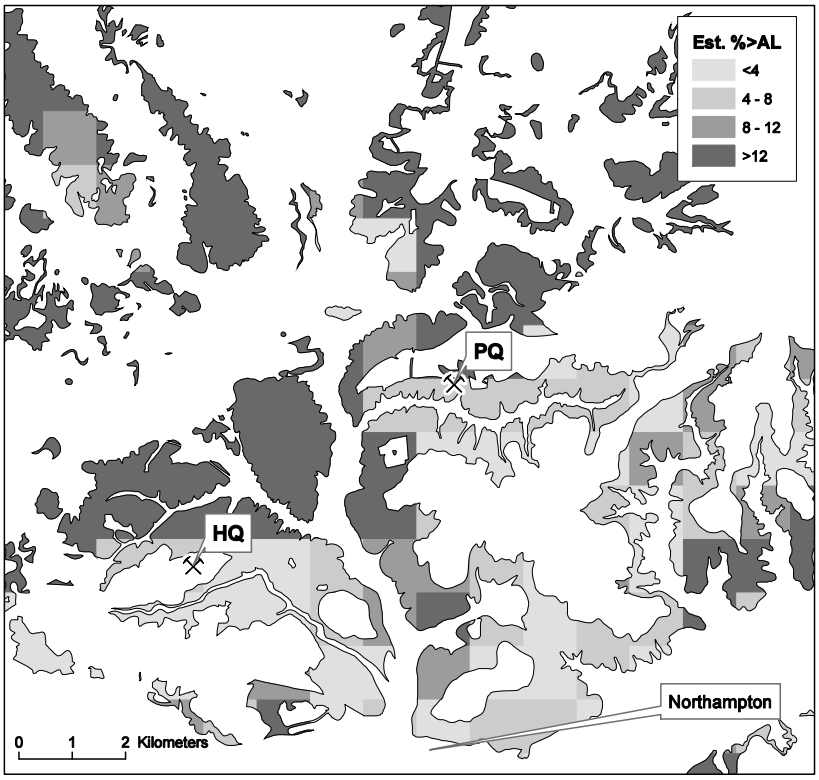

Figure 9. Radon potential of ground underlain by the Northampton Sand Formation (but not covered by superficial deposits) in the Northampton area (HQ = Harlestone Quarry; PQ = Pitsford Quarry). Map based on geology and indoor radon measurements.

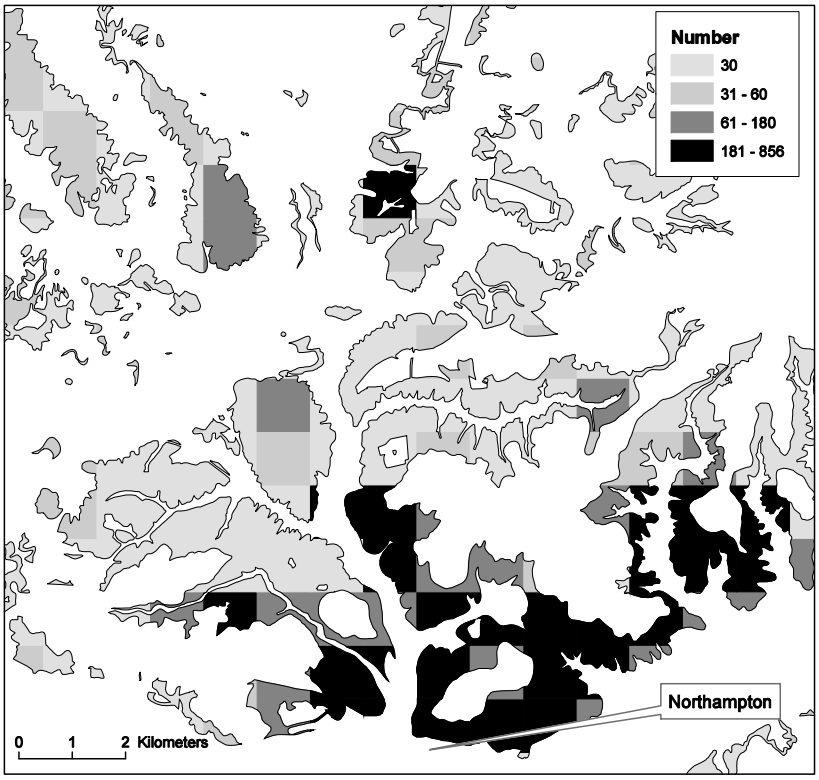

Figure 10. Number of indoor radon measurements used to estimate radon potential in each 1 km grid square underlain by the Northampton Sand Formation (but not covered by superficial deposits) in the Northampton area. Map based on geology and indoor radon measurements.

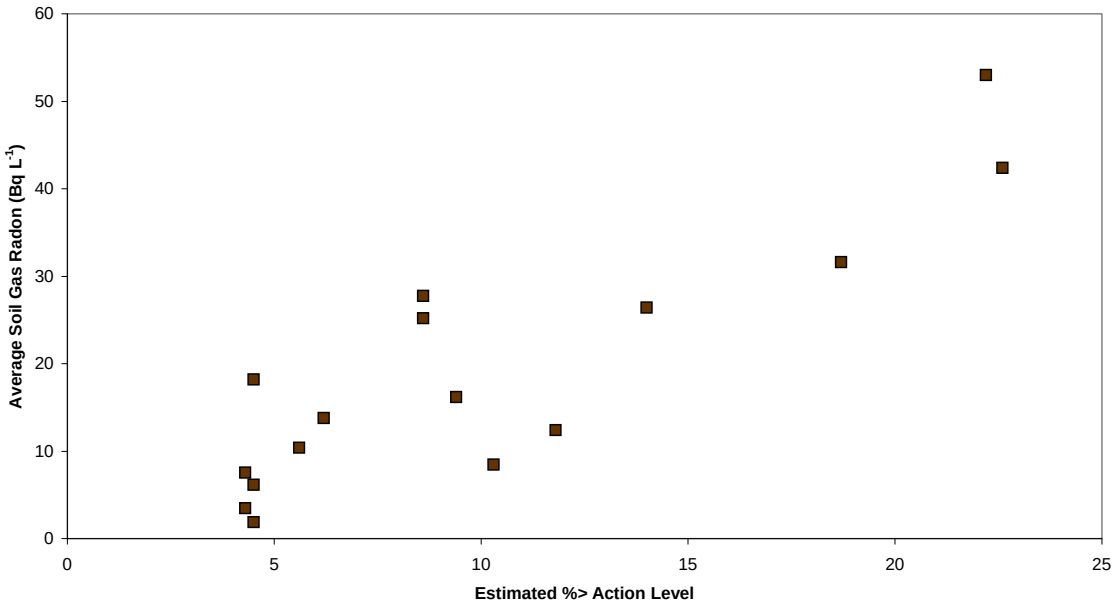

Figure 11. Relationship between average soil gas radon concentration (Bq L^{-1}) and the geological radon potential (Estimated proportion of dwellings exceeding the UK radon Action Level (200 Bq m^{-3})) for the Northampton Sand Formation. Data grouped by 5 km grid square (redrawn after Figure 3-28 in Appleton et al, 2000).

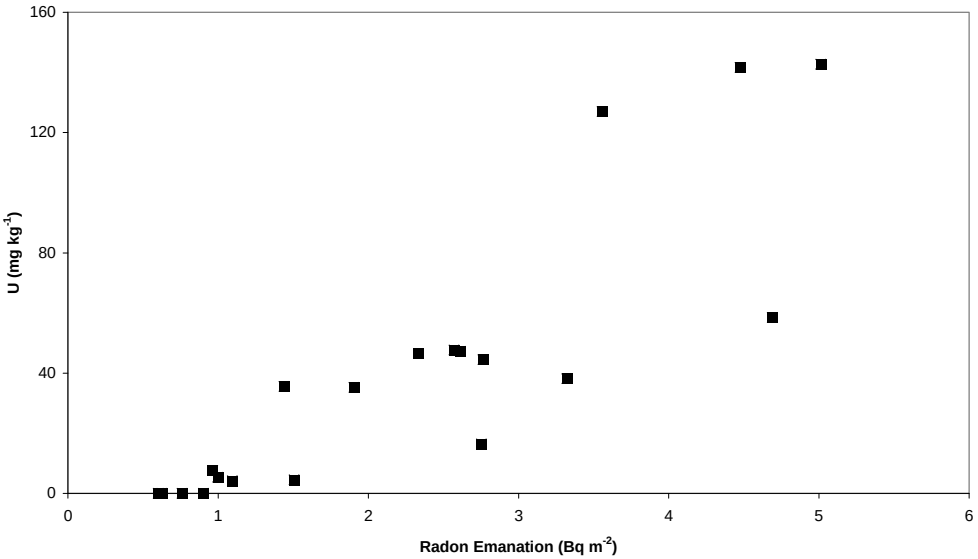

Figure 12. Relationship between radon emanation and uranium concentration of rock samples from the Northampton Sand Formation (Hodgkinson et al 2005)

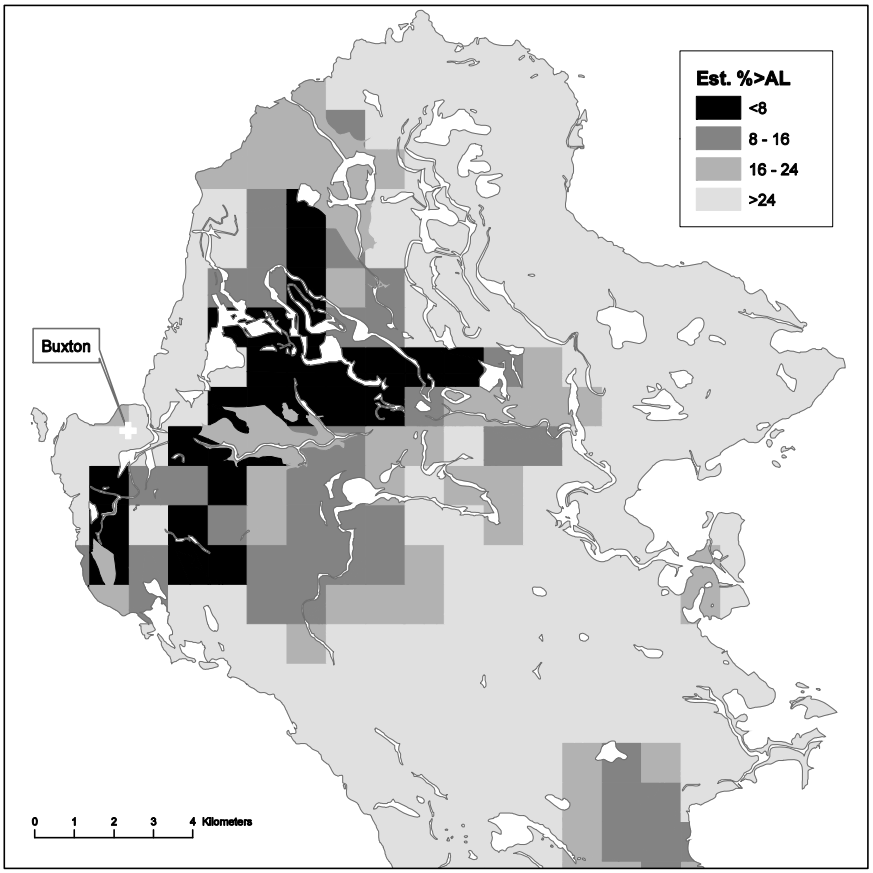

Figure 13. Radon potential map of the northern part of the Derbyshire Dome underlain by Carboniferous limestone, not covered with superficial deposits. Map based on geology and indoor radon measurements.

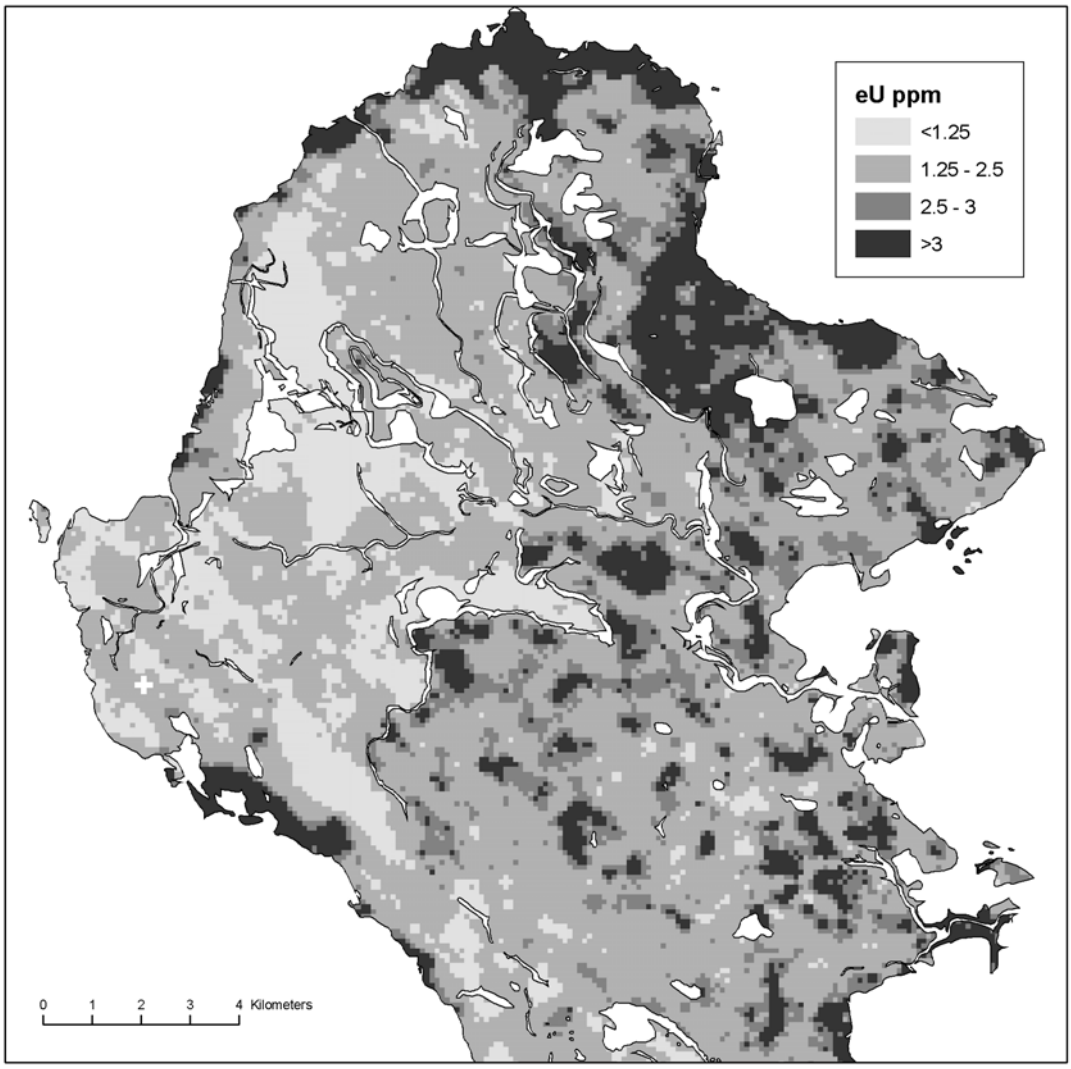

Figure 14. eU (ppm) map of the northern part of the Derbyshire Dome underlain by Carboniferous limestone, not covered with superficial deposits. Data from Hi-RES-1 airborne gamma spectrometry survey (Jones et al 2005)

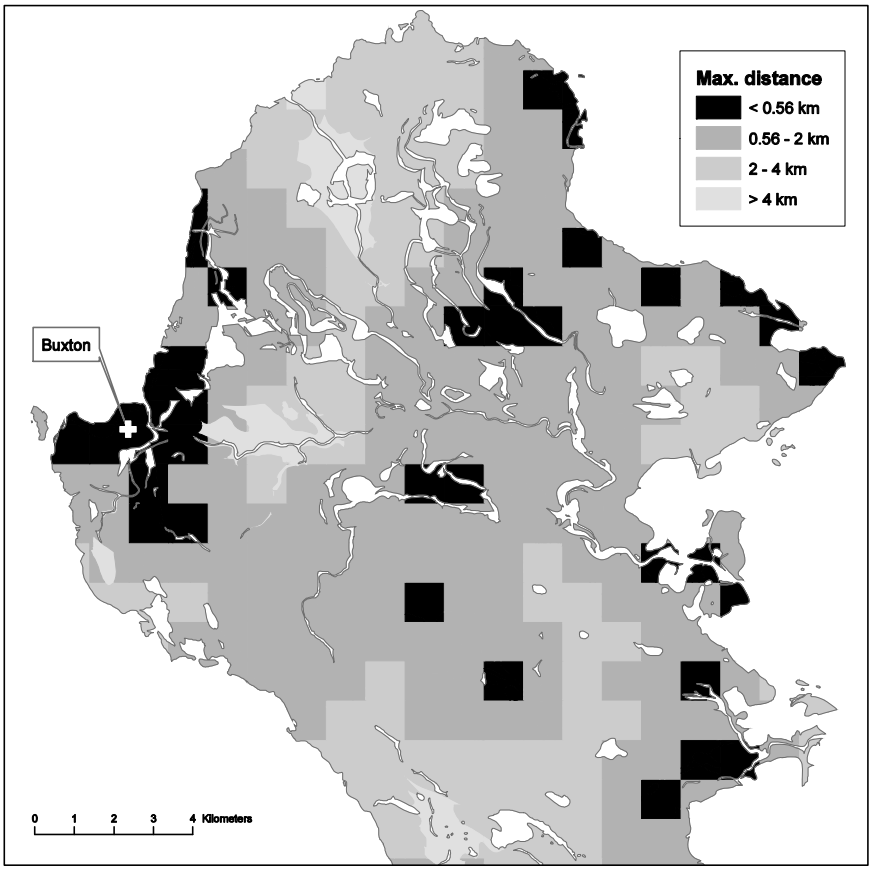

Figure 15. Maximum distance to furthest of 30 measurements used to estimate the radon potential for Carboniferous limestone with no superficial cover, northern sector of the Derbyshire Dome (max. distance <0.56 km indicates that 30 or more measurements occur within the 1 km grid square).

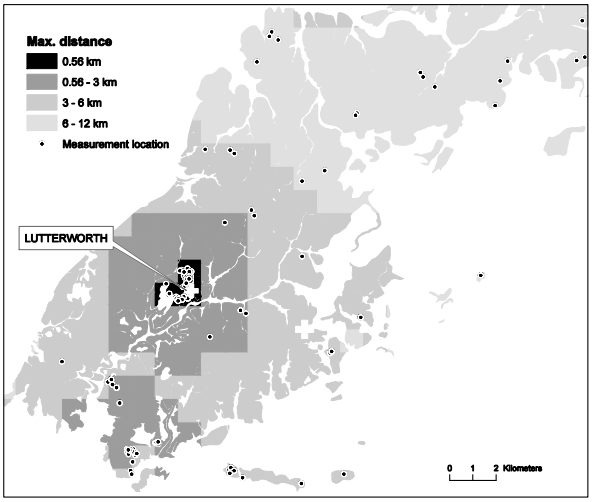

(a)

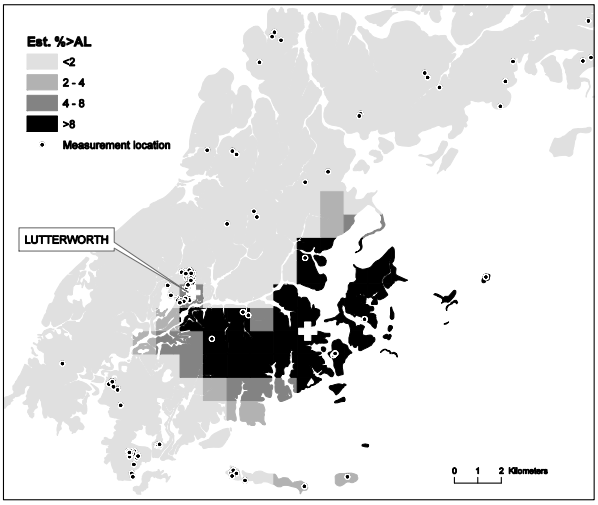

(b)

Figure 16. (a) Indoor radon measurement locations and maximum distance to furthest of 30 measurements used to estimate the radon potential for glacial till overlying Lower Lias bedrock (max. distance <0.56 km indicates that 30 or more measurements occur within the 1 km grid square); (b) radon potential map for glacial till overlying Lower Lias bedrock in the Lutterworth area (map based on geology and indoor radon measurements).